

## BUILDING MECHANICS

UDC 621.791

*Voronezh State University of Architecture and Civil Engineering  
Ph. D. in Engineering, Assoc. Prof. of Dept. of Building Technics  
and Engineering Mechanics A. V. Chernykh*

*D.Sc. in Engineering, Prof., head of Dept. of Organization of Construction, Examination and  
Management of Real Estate V.Ya. Mischenko*

*D.Sc. in Engineering, Prof., head of Dept. of Real Estate Cadastre,  
Land Management and Geodesy V.N. Barinov*

*Russia, Voronezh, tel.: (473)271-59-18;  
e-mail: alexander.v.chernyh@gmail.com*

A. V. Chernykh, V.Ya. Mischenko, V.N. Barinov

### PECULARITIES OF MELTING AND MOVEMENT OF AN ELECTRODE METAL IN ARC WELDING IN AN EXTERNAL CONSTANT LONGITUDINAL MAGNETIC FIELD

**Statement of the problem.** Melting and transfer of electrode metal through the arc are one of the most important technological factors of welding. It is essential to consider the problems associated with the melting of an electrode metal as well as the methods used in this field. Also, considerations should be made of the practical ways of the implementation aimed at the development of an efficient welding technology, especially that of construction metal structures.

**Results.** Principal factors affecting the speed of an electrode melting in arc welding are considered. It is shown that the application of an external magnetic field in welding increases the efficiency of an electrode melting at a constant electric power rate. Shape and sizes of an electrode drops in a magnetic field are experimentally and theoretically determined. The chemical composition and mechanical properties of welding joints are experimentally determined. The practical guidelines on the development of technological modes of welding, particularly in the production of steel bridge structures are formulated.

**Conclusions.** A mathematical model proposed and experimental data on melting and transfer in an electrode metal allows us to make the conclusions about a potentially beneficial use of external magnetic fields in arc welding of building metal structures.

**Keywords:** arc welding, external constant longitudinal magnetic field, melting of an electrode, drop, characteristics of welding joints, steel welded bridge structures.

#### Introduction

A lot of research has been done into the effects of external electromagnetic fields on welding processes (e.g., [1—5]).

The analysis of the research showed that the mechanism of the effect of a magnetic field on the transfer of an electrode metal, kinetics of the melting of an electrode has not been studied and current ideas and perceptions associated with the issue are largely qualitative.

This is mostly due to the complexity involved with studying the melting processes in an electrode in the immediate welding (frequent detachments of drops and the arc temperature of about 6000 to 10000 °C, a variety of acting forces, effect of an electromagnetic field on a liquid electrode metal etc.). Insufficient experimental material has been a hindrance to the qualitative characteristics of phenomena.

This paper seeks to summarize the known results, study the mechanism of the effect of an external longitudinal magnetic field on the kinetics of the melting of an electrode and transfer of drops through an electric arc, investigate the efficiency of the melting of an electrode wire, carry out a comparative study of the chemical composition and mechanical properties of welded joints, provide practical guidelines for the application of magnetic fields while developing welding modes in the building industry.

## **1. Major factors behind the melting rate of the electrode metal**

The nature of the melting and transfer of an electrode metal through the electric arc has a huge influence on enthalpy, temperature of the drops, efficiency of welding, the course of metallurgical reactions [1, 6—10]. It determines the stability of the process, metal loss, joint formation and other technology factors.

Lifespan and sizes of the drops have a significant effect on the heat transfer from an active arc spot to the solid electrode metal.

A mathematical model is presented which describes the dependence between melting rate  $V_{cp}$  of the electrode in non-consumable welding and base characteristics of drop transfer: detachment rate and thickness of a droplet.

The calculations were made according to the scheme specified experimentally in [1, 6, 7] (Fig. 1).

The formation and detachment of the drop from the electrode has a linear periodical nature with triangle signals in the range of  $0 < t \leq T$ :

$$\delta(t) = \frac{\delta}{T}t + \delta_0, \quad (1)$$

where  $\delta$  and  $\delta_0$  is the thickness of the detached and base drop respectively;  $T$  is the period of the formation of the drop;  $t$  is the current time.

Using the condition of the periodicity of the process, a ratio for the average melting rate of the electrode can be obtained:

$$V_{cp} = \sqrt{2\delta}v. \quad (2)$$

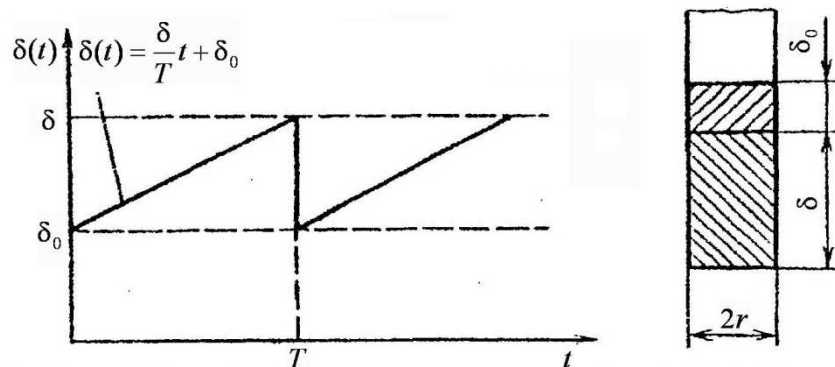


**Fig. 1.** Calculation scheme for average melting rates of the electrode

In order to verify the experimentally obtained dependence high-speed film footage of the electrode melting from the melting wire CB-08A with the diameter of 2 mm in argon [7] was made with the help of an original welding burner [11].

The results of the experimental study of the drop transfer as well as the calculation data in the ratio (2) are in Table 1. The design values of the average melting rate  $V^p$  of the electrode are in good agreement with the experimental results  $V^p$ .

According to [12], the heat conductivity of molten metal rapid drops by 30-40 % compared to the heat conductivity of the same metal in the molten state. An electrode metal drop is therefore a heat-insulating layer that prevents the heat from transferring from the arc to the solid metal electrode. It is thus necessary in melting arc welding to reduce the time a drop is in the end and simultaneously increase the sizes of the transferred drops.

Table 1

The detachment rate and comparative melting rates of the electrode  
(experimental and design ones)

$\delta$ , mm	$v$ , 1/sec	$V^p$ , m/h	$V^p$ , m/h
Reverse polarity			
1.95	11	99	109
0.78	29	107	115
0.59	43	125	129
0.48	58	135	141
Direct polarity			
2.45	19	215	226
1.39	32	232	236
1.12	47	250	267
1.00	64	295	325

## 2. Determining the shape of a free surface of the electrode droplet in a stable longitudinal magnetic field and melting coefficient of the electrode metal

During a welding process taking place in the external magnetic field heat transfer from the arc through a molten drop to the electrode solid metal changes [7]. The high-speed film footage showed that a drop at the end of the electrode starts rotating affected by the electromagnetic forces and takes the shape of a flat rotational ellipsoid. The rotation time and its thickness on the end of the electrode decrease as the induction of the magnetic field is on the rise (Fig. 2).

The maximum detachment rate is 60 Hz in the induction of the magnetic field in the welding area of about 50 mT. Further increase in the induction of the magnetic field has no effect on the melting rate of the electrode [10].

In order to give a mathematical description of the shape and physical processes taking place in the rotating droplet (Fig. 3), let us write the Euler equation as a projection of mass forces onto the Oxyz coordinates:

$$X = \omega^2 x, Y = \omega^2 y, Z = -g \frac{z}{R},$$

where  $\omega$  is the angular rotation speed of the drop;  $X, Y, Z$  are projections of the forces onto the coordinates;  $x, y, z$  are current axis of the point in question within the drop.

The pressure of the mass forces that affect the elementary volume of the rotating drop is given by the equation

$$dP = (Xdx + Ydy + Zdz)\rho,$$

where  $\rho$  is the density of the molten metal electrode.

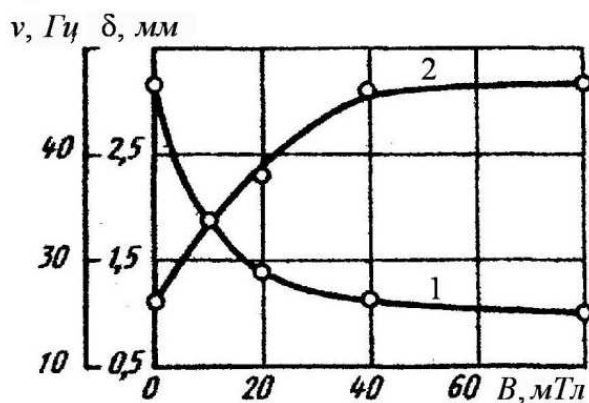


**Fig. 2.** Dependence of the maximum thickness of a molten layer  $\delta$  on the end of the electrode (1) and drop transfer rate  $v$  (2) on the induction of the magnetic field

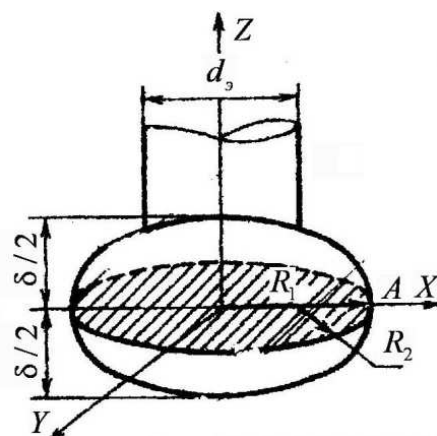


**Fig. 3.** Schematic of a drop rotating on the end of the electrode in the longitudinal magnetic field

Following the integration of the Euler equations, the general solution looks as follows

$$P = \frac{1}{2} \left( \omega^2 x^2 + \omega^2 y^2 - \frac{g}{R} z^2 \right) \rho + C. \quad (3)$$

The expression (4) is the equation of the flat rotational ellipsoid [7].

Equation (3) yields the ratio [7] for the thickness of a molten drop on the end of the electrode:

$$\delta = \sqrt[3]{\frac{8\pi\sigma}{IB}} r. \quad (4)$$

In order to determine the productivity of the electrode metal welding in the longitudinal magnetic field, it is necessary that heat losses in the molten droplet are known.

Let us examine the heat balance equation in the phase transition (Stefan problem) assuming that in the first phase the temperature in the droplet is given by the following conditions: on the surface of the phase transition to the solid to molten metal it is abtained at the welding temperature (1812°K). On the droplet surface (liquid-gas phase transition) from the arc it is equal to the boiling temperature which is 3013 °K.

Besides, let us assume that within the droplet the temperature is distributed linearly [13].

According to the heat transfer equation from the arc to the electrode [14], we can write:

$$q_1 - q_2 = c \int_0^{\delta} (T(z) - T_{nl}) dz + Q_{nl} \delta, \quad (5)$$

where  $q_1 = \eta UI$  and  $q_2 = \pi r_s^2 V c_p T$  are densities of the heat flux coming and going out of the droplet respectively, Watt sec/m<sup>2</sup>;  $c$  is the specific heat capacity, J/kg K;  $Q_{nl}$  is the latent melting heat, J/kg;  $\eta$  is the coefficient of the efficiency of the power supply of the electric welding arc;  $U$  is the arc voltage (35 W);  $V = \alpha_p I / \pi \rho r_s^2$  is the melting rate of the electrode;  $\alpha_p$  is the melting coefficient of the electrode metal, g/A h.

Following the integration of (5) considering [13] and simple transformations, we get the expression for the melting coefficient of the electrode metal  $\alpha_p$ :

$$\alpha_p = \frac{\eta UI - c\delta(T_{\text{кин}} - T_{\text{нл}}) \frac{2\sqrt{\delta^2 + r_0^2} - \delta}{2\sqrt{\delta^2 + r_0^2}} - Q_{\text{нл}} \delta}{cI\Delta T}, \quad (6)$$

where  $\Delta T$  is the average temperature of the droplets [13].

The calculation results for the thickness of the molten drop  $\delta$  and melting coefficient of the electrode metal  $\alpha_p$  in comparison with the experimental data are identified in Table 2. The results below show the calculation results are consistent with the experimental data.

Table 2

Dependence of the thickness of the droplet and melting coefficient on the induction of the magnetic field

Induction of the magnetic field in the droplet, W mT	Thickness of the droplet $\delta$ , mm		Melting coefficient $\alpha_p$ , g/A h	
	calculational	experimental	calculational	experimental
25	1.8	1.9	8.9	12.0
55	1.3	1.4	12.0	13.4
110	1.1	1.1	13.3	14.4
140	1.0	1.0	13.9	14.8

**Note:** welding current is 225 A; surface tension coefficient is 1.2 N/m; electrode radius is 1 mm.

### 3. Experimental study of the shape of the droplet and melting rate of the metal electrode in arc welding in the external longitudinal magnetic field

The melting rate of the electrode wire with the diameter of 2 or 5 mm was investigated in automatic flux-cored welding in the current range of 200—1000 A. The melting rate was esti-

mated using the melting coefficient  $\alpha_p$ . The study was carried out by welding of 10XCHД steel plates of 12×200×500 mm used in bridge construction with the help of АДФ-1002 and АН-248А flux-cored СВ-08А wire. The external longitudinal magnetic field was generated in the weld fusion using an electric magnet fitted on the welding end in alignment with the electrode wire [11]. The induction of the magnetic field varied in the range of 0 to 100 mTesla.

For the specified current the wire was supplied at the rate that would ensure a stable weld fusion and the voltage was measured. After the magnetic field was switched on, the melting rate of the electrode started to increase which resulted in a longer arc and greater voltage with the current decreasing respectively and the rate at which the wire was supplied was therefore increased causing the arc voltage and current to reach their initial values.

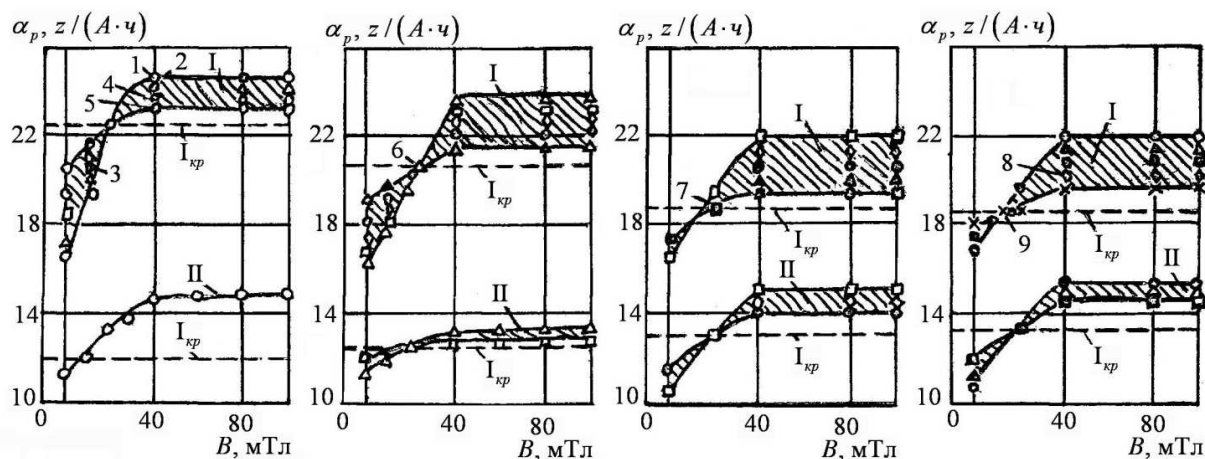
The mass of the welded electrode wire was identified as the difference between the results of its weighing before and after the welding. The productivity of the electrode welding was assessed using the melting coefficient  $\alpha_p$ , g/A h:  $\alpha_p = m/It$  where  $m$  is the mass of the melted wire over the time  $t$ ;  $I$  is the welding current, A.

The results of the study are identified in Fig. 4 and 5 that indicate that in the external longitudinal magnetic field the melting rate of the electrode wire increases while the arc power supply rebases unchanged. The induction up to 40 mT shows an almost linear growth of the productivity of the melting of the electrode wire (a further induction increase has no effect on the productivity).

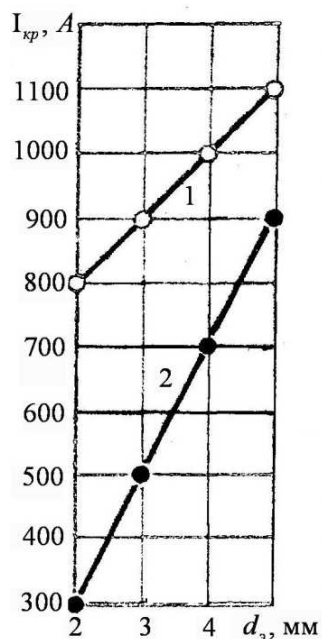
The melting rate is mostly influenced by the magnetic field at the direct current (up to 50 %) and is least influenced at reverse current (25—30 %). When the arc was supplied with an alternating current, the electrode wire performance was 10—12 % higher than with the constant reverse current. The experimental results are consistent with the previously made assumption on the magnetic field being conducive to the improvement of the heat productivity observed in the active spot.

Fig. 4 shows the experimental dependencies of the melting coefficient of the electrode wire on the induction of the external longitudinal magnetic field for different welding currents and electrode diameters. During the welding with the inductions of the magnetic field ranging up to 40 mT, the rate of the coefficient growth decreases as the magnitude of the welding current

increases, which causes the intersection point to appear. As the welding current hits some value which is called a critical one, the magnetic field does not influence  $\alpha_p$  any longer since the globular transfer means a high productivity of the electrode melting which relates to the horizontal dashed line in the graphs in Fig. 4.



**Fig. 4.** Dependence of the melting coefficient of the electrode wire on the induction of the longitudinal magnetic field for different diameters of the electrode:  
 a — d is the diameter of the electrode 2, 3, 4 and 5 mm respectively;  
 1—9: I is 200, 300, 400, 500, 600, 700, 800 and 900 A respectively;  
 I, II is the direct and reverse polarity



**Fig. 5.** Dependence of the critical welding current on the diameter of the electrode wire: 1 is the direct polarity; 2 is the reverse polarity

Excessive critical currents are accompanied by a transition from the droplet to flux transfer of the electrode metal. No effect of the magnetic field on the coefficient  $\alpha_p$  is caused by a change of the nature of the droplet transfer.

Its critical values resulting from direct and reverse current welding that make the magnetic field no longer affect the productivity of the melting of the electrode wire are graphically presented in Fig. 5. These dependencies are linear.

A longitudinal magnetic field is more advisable to be used for when extra weld metal is necessary in the joint (for the edges of joints, welding works, angular joints, etc.), e.g., in bridge construction.

#### **4. Influence of the external longitudinal magnetic field on the composition of the welded metal joint.**

During flux-cored welding the rotation of the droplets increases the time and area of the interface of the molten metal and flux which gives rise to more alloying elements in the joint metal. This is why the chemical composition of the welded joints carried out using a conventional technology [15] (mode № 1) and joints obtained in the longitudinal magnetic field (mode № 2—4).

The angular joints were carried out with 7 mm cathetuses of 10XCHД steel welded alloys in the lower position with a 5 mm CB-08ГA wire using AH-348A flux with 41—44 % SiO and 34—38 % MnO. A constant magnetic field was generated using an electric magnet [11]. Welding modes in the magnetic field (Table 3) reverse currents were selected according to [10, 15] while the ratios of the base and electrode metal rebases unchanged.

The distribution of Cr and Mn in the metal joint were investigated using the local X-ray spectrum analysis. The research suggests that in welded alloys these elements were distributed evenly along the entire joint. Further on, the quantitative values of the alloy elements Cr, Mn, Ni, Si, Cu as well the harmful sulphur impurity were calculated with the help of the spectrum method. The amount of C and S were determined by burning of chips in the oxygen flow followed by the estimation of the carbon gas and sulphurous antihydride using an infrared cell. The results of the research are in Table 4.

Table 3

## Welding modes

Mode number	Induction of the magnetic field, mT	Melting rate of the electrode, m/h	Welding rate, m/h
1	0	72.5	46
2	10	78.0	51
3	30	85.0	55
4	40	91.0	59

Here is the calculated chemical composition of the metal joint. The elements  $[\mathcal{A}]_p$  in the joint are given by the expression:

$$[\mathcal{A}]_p = [\mathcal{A}]_o m + [\mathcal{A}]_e n,$$

where  $[\mathcal{A}]_o$  and  $[\mathcal{A}]_e$  are the amounts of the component in the base and electrode metals respectively;  $m = 0.6$ ,  $n = 0.4$  are the amounts of the base and electrode metals in the joint.

The actual amount of C, Cr, Ni, Cu in the metal joint during ordinary welding is smaller than the computational one (Table 4) which is obviously caused by burning-out of the above elements under the action of the electric arc.

During the magnetic pulse welding (Table 4) the amount of the elements in the metal joint increases and approaches the computational value as so does the induction. First of all, this is caused by a larger melting rate of the electrode which results in the overheating of the droplet and burning out of alloy elements. Secondly, the centrifugal force gives rise to the split of the electrode droplets that result in the increasing time and area of the interface of the molten metal and the flux. Thirdly, alignment of the temperatures of the axial and periphery areas in the welded metal due to the rotation [16] promotes blending and cooling of the latter. The amount of  $S$  does not almost change as the induction of the magnetic field increases.

Table 4

Computational and experimental amount of alloy elements in the metal joint depending on the induction of the magnetic field

V, mT	Amount of the elements, %						
	C	Si	Mn	Cr	Ni	Cu	S
Experimental values							
0	0.06	0.50	0.92	0.40	0.10	0.32	0.030
10	0.08	0.50	0.94	0.42	0.12	0.32	0.018
30	0.08	0.55	0.99	0.47	0.20	0.36	0.015
45	0.08	0.60	1.00	0.48	0.23	0.35	0.020
Computational values							
-	0.10	0.49	0.80	0.47	0.34	0.30	0.018

The distribution of microsolidity across the alloy joint carried out in an ordinary welding in the magnetic field. Microsolidity of the specimens in the welded alloy areas is not much different and is 2500—2700 MPa for the base metal, 3000—3300 MPa in the vicinity of the joint, 2800—3000 MPa for the joint metal.

The sizes of the metal grain in the vicinity of the joint is 4.5—9.0 mkm and 18—22 mkm in the base metal.

### 5. Mechanical properties of welded alloys in the longitudinal magnetic field welding

Comparative research of T-shaped alloys welded in the longitudinal magnetic field using an ordinary technology. That was mechanic welding in the plant manufacture of steel bridge structures [15]. For this purpose specimens were made from a 12-mm sheet steel 10XCHД

using automatic AH-348AM flux-cored welding (electrode wire CB-08A with the diameter of 2 mm). Angular single-pass joints with 6 mm cathetuses using a welding machine АДФ-1002. The arc was power supplied by reverse current from a wire feeder BC-600.

The limit of fluidity  $\delta_T$  and strength  $\sigma_B$ , relative extension  $\delta_{10}$  was determined using a standard method on the tensile machine with the tension of no less than five specimens (Table 5).

Table 5

## Comparative mechanical properties of welding joints

Welding	Melting rate of the electrode, m/h	Induction of the magnetic field, mT	Welding rate, m/h	$\delta_T$ , MPa	$\sigma_B$ , MPa	$\delta_{10}$ , %
According to the plant specifications [11]	146	-	26	545	625	24
In the longitudinal magnetic field	250	50	36	520	660	24
In modes specified in the instructions [11]				$\geq 325$	$\geq 470$	$\geq 16$

The strength HV of the base metal is 158 and for the joint metal is 177 and 186, and in the vicinity of the joint is 177 and 200 according to the plant specifications in the magnetic field respectively. In the modes specified in the instruction [15] the strength should be more than 350 HV.

Mechanical properties of 10XCHД steel T-shaped joints produced according to both of the technologies are completely in accordance with the industry specifications [15]. It is therefore to be noted that the melting rate in the magnetic field is 38 % higher. Structural components of the joint metal and in the vicinity of the joint as well as the extension of the latter in the

weld specimens are quite identical. However, the joint metal crystallized in the longitudinal magnetic field has a more fine-grained structure [17].

The tensile tests were carried out at the loading of 10 Hz in 2000000 cycles and asymmetry coefficient of the cycle of 0.25, which is in accordance with the actual operation of bridge structures. The regressive analysis found the linear dependence between the logarithm of the number of the cycles  $N$  prior to the failure and maximum strain  $\sigma_{\max}$  of the cycle (Fig. 6). The results of the tensile tests show that the durability of the welding alloys made in the longitudinal magnetic field is on average 5—10 % higher than that of the alloys made in accordance with the plant specifications [15].

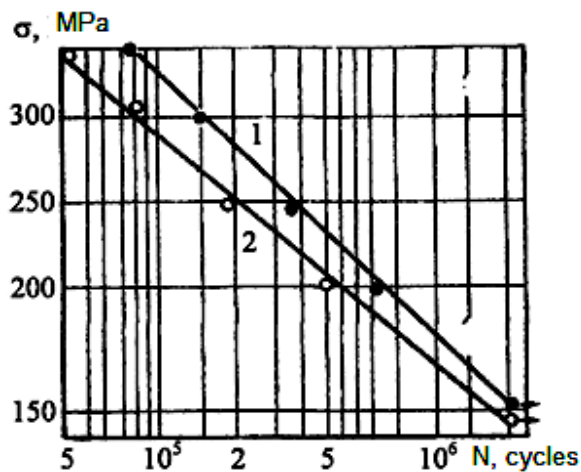


**Fig. 6.** Results of the tensile tests:  
1 is the welding in the longitudinal magnetic field; 2 is in accordance with the plant specifications [15]

A rise in the resistance to tension in T-shaped joints of bridge structures during magnetic field welding is due to the conditions giving rise to the formation of a joint, high amount of alloying elements [9] as well as a fine-grained disoriented structure of the crystals.

## Conclusions

1. It was experimentally and theoretically found that an average melting rate of the electrode is determined by the frequency and size of the transferred droplets.
2. A longitudinal magnetic field improves the productivity of melting of the electrode metal in arc welding. The maximum increase in the melting coefficient is 50 % (30 %) in direct current reverse polarity welding and is 40% for alternating polarity welding.

3. The obtained experimental dependencies are consistent with the theoretical calculations and permit to determine a necessary melting rate of the electrode wire using the longitudinal magnetic field in the development of technological processes in the welding arc and in particular welding of steel bridge structures.

4. In welding in the longitudinal magnetic field as a result of less great burning and more intense chemical reactions taking place between the molten metal and the flux there is alloy enrichment of the joint metal which should promote technological and mechanical properties of welding joints.

5. In magnetic field welding as a result of less great burning and more intense chemical reactions between the molten metal and the flux there is alloy enrichment of the joint metal which should promote technological and mechanical properties of welding joints.

6. The comparative research suggests higher properties of welded joints carried out in the longitudinal magnetic field compared to the similar specimens welded according to the traditional technology.

Despite a great number of publications [1—17, etc.] and stable analysis, potential importance as well as the examined physical and chemical phenomena taking place in the vicinity of the triple point are the reason why the field needs further scientific and practical attention.

#### References

1. **Erokhin, A. A.** Osnovy svarki plavleniem / A. A. Erokhin. — M.: Mashinostroenie, 1973. — 448 s.
2. **Gagen, Ju. G.** Svarka magnitoupravljaemojj dugojj / Ju. G. Gagen, V. D. Taran. — M.: Mashinostroenie, 1970. — 160 s.
3. **Kompan, Ja. Ju.** Ehlektroshlakovaja svarka i plavka s upravljaemymi MGD-processami / Ja. Ju. Kompan, Eh. V. Shherbinin. — M.: Mashinostroenie, 1989. — 272 s.
4. **Erdmann-Jesnitzer, F.** Beobachtungen zur Wirkung von Magnetffedern beim

Lichtbogenschweissen / F. Erdmann-Jesnitzer, W. Schroder, J. Schubert // Werkstatt und Betrieb, 94/ Jahrg/ 1961. Helf 8. — S. 506—508.

5. **Svarka s ehlektromagnitnym peremeshivaniem** / pod obshh. red. V. P. Chernysha; Kiev: Tekhnika, 1983. — 128 s.

6. **Boldyrev, A. M.** Vlijanie osnovnykh kharakteristik kapleperenosa na srednjuju skorost' plavljenija ehlektroda / A. M. Boldyrev, V. A. Birzhev, A. V. Chernykh // Svarochnoe proizvodstvo. — 1995. — № 1. — S. 6—8.

7. **Boldyrev, A. M.** Osobennosti plavljenija ehlektrodnogo metalla pri svarke vo vneshnem prodol'nom magnitnom pole / A. M. Boldyrev, V. A. Birzhev, A. V. Chernykh // Svarochnoe proizvodstvo. — 1991. — № 5. — S. 28—30.

8. **Chernykh, A. V.** Opredelenie uglovojj skorosti vrashhenija kapli na torce ehlektroda pri dugovojj svarke v magnitnom pole / A. V. Chernykh, V. V. Chernykh // Svarochnoe proizvodstvo. — 2010. — № 7. — S. 8—10.

9. **Boldyrev, A. M.** Vlijanie vneshnego prodol'nogo magnitnogo polja na sostav naplavlennogo metalla shva / A. M. Boldyrev, V. A. Birzhev, A. V. Chernykh // Svarochnoe proizvodstvo. — 1993. — № 8. — S. 28—30.

10. **Boldyrev, A. M.** Povyshenie proizvoditel'nosti rasplavljenija ehlektrodnoj provoloki pri svarke v prodol'nom magnitnom pole / A. M. Boldyrev, V. A. Birzhev, A. V. Chernykh // Svarochnoe proizvodstvo. — 1989. — № 4. — S. 18—19.

11. **A. s. 1382614 SSSR, MKI V 23 K 9/08.** Gorelka dlja svarki magnitoupravljaemojj dugojj / A. M. Boldyrev, V. A. Birzhev, A. V. Chernykh (SSSR). — № 4019054/31-27; zajavl. 11.02.86; opubl.23.03.88, Bjul. № 11. — 2 s.

12. **Zhdanov, G. S.** Fizika tverdogo tela / G. S. Zhdanov. — M.: Izd-vo MGU, 1962. — 397 s.

13. **Chernykh, A. V.** Raschet temperatury ehlektrodnykh kapel' pri dugovojj svarke plavjashhimsja ehlektrodom s pomoshh'ju metoda konechnykh ehlementov / A. V. Chernykh, V. V. Chernykh // Svarochnoe proizvodstvo. — 2008. — № 3. — S. 6—7.

14. **Muchnik, G. F.** Metody teorii teploobmena: v 3 ch. Ch. 1. Teploprovodnost' / G. F. Muchnik, I. B. Rubashov. — M.: Vyssh. shk., 1970. — 288 s.
15. **VSN 169-80.** Instrukcija po tehnologiji mekhanizirovannoj i ruchnoj svarki pri zavodskom izgotovlenii stal'nykh konstrukcij mostov. — M.: Mintransstrojj, 1981. — 86 s.
16. **Chernykh, A. V.** K ocenke uglovoj skorosti vrashhenija zhidkogo metalla pri dugovoj svarke v postojannom prodol'nom magnitnom pole / A. V. Chernykh, V. V. Chernykh // Izvestija vuzov. — 2011. — № 10. — S. 108—111.
17. **Boldyrev, A. M.** Svojjstva soedinenij iz stali 10KhSND pri svarke v prodol'nom magnitnom pole / A. M. Boldyrev, V. A. Birzhev, A. V. Chernykh // Svarochnoe proizvodstvo. — 1990. — № 9. — S. 8—9.